P1.5 A BULK AIR-SEA FLUX ALGORITHM FOR HIGH-WIND, SPRAY CONDITIONS, VERSION 2.0

Edgar L Andreas*
U.S. Army Cold Regions Research and Engineering Laboratory, Hanover, New Hampshire

1. INTRODUCTION

In high winds, spray processes could conceivably dominate the exchange of sensible heat, latent heat, and momentum across the air-sea interface (Emanuel 2003; Andreas 2004). In low winds, on the other hand, when spray droplets are not plentiful, the exchange of heat and momentum across the air-sea interface is strictly by interfacial processes that the COARE algorithm (Fairall et al. 1996) does well in predicting.

In the last conference in this series, I introduced Version 1.0 of a bulk flux algorithm that merges these two extremes (Andreas 2003). It relied on the COARE algorithm to predict the interfacial fluxes of sensible heat, latent heat, and momentum but included a spray parameterization to account for how sea spray could enhance the heat fluxes in high winds. We soon realized, however, that the spray component of that algorithm was not sensitive enough to temperature (Li et al. 2003) and that it also had flaws at very high relative humidity. Here I address these shortcomings with Version 2.0 of a bulk flux algorithm for high-wind, spray conditions.

2. THE INTERFACIAL FLUXES

Traditional bulk flux algorithms predict only the interfacial fluxes of momentum (τ, also called the surface stress), sensible heat (H_s), and latent heat (H_L) through

$$\tau \equiv \rho u_*^2 = \rho C_{Dr} U_r^2 , \qquad (1a)$$

$$H_s = \rho c_p C_{Hr} U_r \left(T_s - T_r\right) , \qquad (1b)$$

$$H_L = \rho L_v C_{Er} U_r \left(Q_s - Q_r\right) . \qquad (1c)$$

In these, ρ is the air density; c_p, the specific heat of air at constant pressure; L_v, the latent heat of vaporization; U_r, T_r, and Q_r, the average wind speed, potential temperature, and specific humidity at reference height r; and T_s and Q_s, the average temperature and specific humidity at the surface. Equation (1a) also defines the friction velocity u_*.

The key to the interfacial bulk flux algorithm is evaluating the transfer coefficients for momentum (C_{Dr}, also called the drag coefficient) and sensible (C_{Hr}) and latent (C_{Er}) heat. These derive from Monin-Obukhov similarity theory (Garratt 1992, p. 52 ff.) and are written formally as

$$C_{Dr} = \frac{k^2}{\left[\ln\left(\frac{r}{z_0}\right) - \psi_m\left(\frac{r}{L}\right)\right]^2} , \qquad (2a)$$

$$C_{Hr} = \frac{k^2}{\left[\ln\left(\frac{r}{z_T}\right) - \psi_h\left(\frac{r}{L}\right)\right]\left[\ln\left(\frac{r}{z_0}\right) - \psi_m\left(\frac{r}{L}\right)\right]} , \qquad (2b)$$

$$C_{Er} = \frac{k^2}{\left[\ln\left(\frac{r}{z_Q}\right) - \psi_h\left(\frac{r}{L}\right)\right]\left[\ln\left(\frac{r}{z_0}\right) - \psi_m\left(\frac{r}{L}\right)\right]} . \qquad (2c)$$

Here, k (= 0.40) is the von Kármán constant; L is the Obukhov length, a stratification parameter; and ψ_m and ψ_h are known functions of the stratification, r/L.

In essence, estimating the interfacial fluxes is a matter of choosing parameterizations for the roughness lengths for wind speed (z_0), temperature (z_T), and humidity (z_Q). I use, basically, the COARE Version 2.6 parameterization (Fairall et al. 1996) for these. Fairall et al. (1996) base z_0 on the sum of Charnock's relation and an aerodynamically smooth relation, as suggested by Zilitinkevich (1969) and Smith (1988),

*Corresponding author address: Edgar L Andreas, U.S. Army Cold Regions Research and Engineering Laboratory, 72 Lyme Road, Hanover, New Hampshire 03755-1290; e-mail: eandreas@crrel.usace.army.mil.

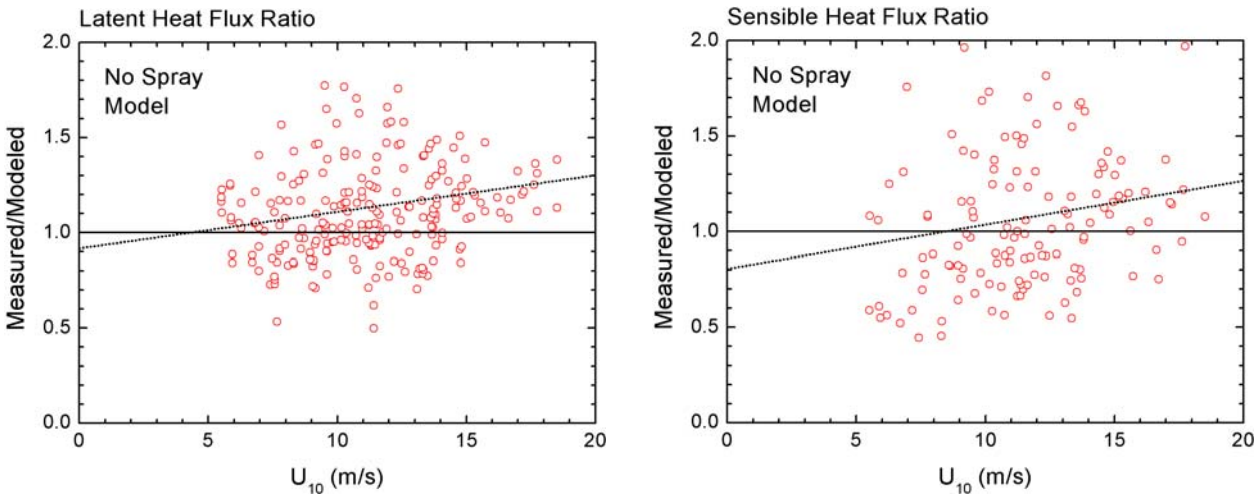

Fig. 1. HEXOS measurements of the latent and sensible heat fluxes are compared with values modeled strictly with the interfacial algorithm, (1)–(2). [That is, $\alpha = \beta = \gamma = 0$ in (4).] If the model were accurate, the ratios depicted would average one and would show no trend with the 10-m wind speed, U_{10}. The dashed lines, however, show the trends with wind speed. In the latent heat flux panel, the ratios average 1.133, and their correlation coefficient with wind speed is 0.184. In the sensible heat flux panel, the ratios average 1.073, and the correlation coefficient is 0.174.

$$z_0 = 0.135\frac{\nu}{u_*} + \alpha_C \frac{u_*^2}{g} , \qquad (3)$$

where ν is the kinematic viscosity of air and g is the acceleration of gravity. I deviate slightly from Fairall et al. by using a somewhat larger coefficient, 0.135, in the aerodynamically smooth term (Andreas and Treviño 2000) and a larger Charnock coefficient, $\alpha_C = 0.0185$, that is probably more appropriate for the younger, rougher sea surface typical under high winds (Wu 1982; Johnson et al. 1998).

The HEXOS data set (DeCosmo 1991; DeCosmo et al. 1996) is one of the better sets for investigating flux parameterizations in high winds. It includes eddy-correlation measurements of the momentum and sensible and latent heat fluxes over the North Sea in 10-m winds up to almost 20 m s^{-1}. Figure 1 shows, however, that the COARE algorithm, represented by (1) and (2), does not do well in predicting the measured HEXOS sensible and latent heat fluxes (cf. Andreas and DeCosmo 1999, 2002). The measured fluxes tend to be increasingly larger than the modeled fluxes as the wind speed increases. Andreas and DeCosmo (2002) interpret this behavior to be evidence of spray-mediated fluxes in the high winds.

3. PARTITIONING THE FLUXES

To represent the spray-mediated fluxes in the HEXOS data, Andreas and DeCosmo (1999, 2002) use Andreas's (1989, 1992) microphysical model to predict the spray latent ($\overline{Q}_L$) and sensible ($\overline{Q}_S$) heat flux contributions and assume that these just add linearly to the interfacial fluxes predicted by (1) and (2);

$$H_{L,T} = H_L + \alpha \overline{Q}_L , \qquad (4a)$$

$$H_{s,T} = H_s + \beta \overline{Q}_S - (\alpha - \gamma)\overline{Q}_L . \qquad (4b)$$

Here, $H_{L,T}$ and $H_{s,T}$ are the total latent and sensible heat fluxes that eddy-correlation instruments would measure just above the droplet evaporation layer (Andreas et al. 1995; Andreas and DeCosmo 2002); and α, β, and γ are small, non-negative constants that tune the model to data.

In (4a), the α term represents the latent heat flux contributed by evaporating spray droplets. This same term must appear with the opposite sign in (4b) because these droplets consume sensible heat to evaporate. The β term in (4b) quantifies the sensible heat that spray droplets give up in cooling from T_s to their respective equilibrium temperatures (e.g., Andreas 1995). Lastly, the γ term in (4b) is a feedback terms; it results because

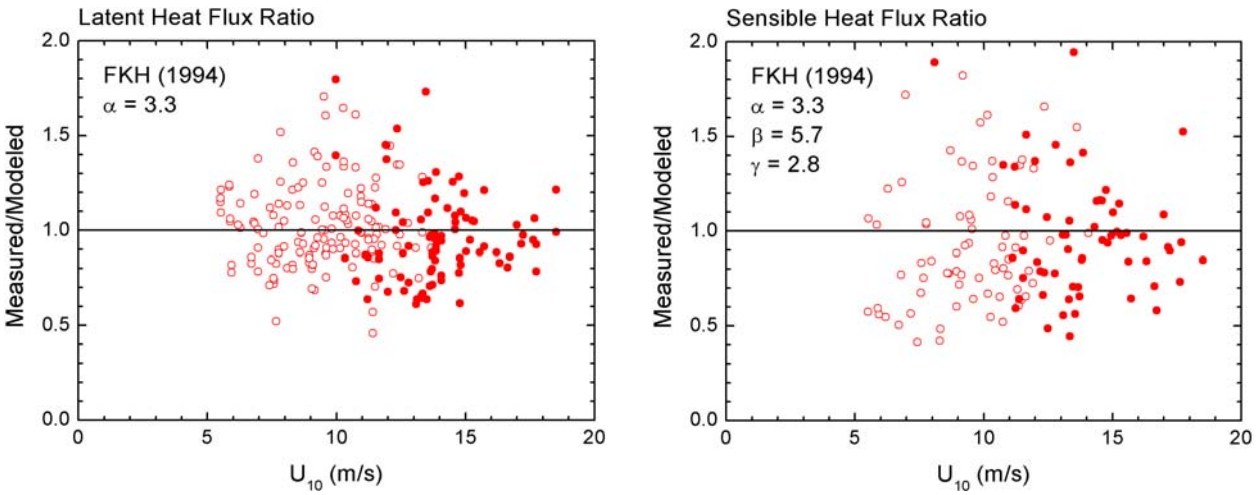

Fig. 2. As in Fig. 1, but here I use (4) to model the HEXOS heat flux data. Equations (5) and (6) use the model by Fairall et al. (1994; FKH) for the spray generation function; and in (4), $\alpha = 3.3$, $\beta = 5.7$, and $\gamma = 2.8$. In the latent heat flux panel, the ratios average 1.025, and their correlation coefficient with wind speed is –0.052. In the sensible heat flux panel, the ratios average 0.984, and the correlation coefficient is 0.044. The filled circles denote cases for which the modeled spray contributions [the α, β, and γ terms in (4)] sum to at least 10% of the respective modeled interfacial fluxes [the H_S and H_L terms in (4)].

the evaporating spray cools the near-surface air and, thus, increases the sea-air temperature difference beyond the difference assumed in (1b) (cf. Katsaros and DeCosmo 1990). I expect $\gamma \le \alpha$.

The $\overline{Q}_L$ and $\overline{Q}_S$ values in (4) come from my microphysical spray model (Andreas 1992). This computes the radius-specific droplet sensible heat flux as

$$Q_S(r_0) = \rho_s c_w (T_s - T_{eq})\left[1 - \exp(\tau_f / \tau_T)\right]\left(\frac{4\pi r_0^3}{3}\frac{dF}{dr_0}\right). \quad (5)$$

Here, ρ_s is the density of seawater; c_w is the specific heat of seawater at constant pressure; T_{eq} is the equilibrium temperature of a saline droplet with initial radius r_0 (a function also of air temperature, relative humidity, and initial salinity; Andreas 1995, 1996; Kepert 1996); τ_T is the e-folding time to reach this temperature; τ_f is related to the droplet's residence time in the air; and dF/dr_0 is the spray generation function, the rate at which droplets of initial radius r_0 are produced at the sea surface.

The radius-specific spray latent heat flux is similar but has two parts. Let τ_r be the e-folding time for a droplet with initial radius r_0 to reach its equilibrium radius r_{eq} (Andreas 1990, 1992). Then, if $\tau_f > \tau_r$, I assume the droplet has reached its equilibrium radius, and

$$Q_L(r_0) = \rho_w L_v \left\{1 - \left(\frac{r_{eq}}{r_0}\right)^3\right\}\left(\frac{4\pi r_0^3}{3}\frac{dF}{dr_0}\right). \quad (6a)$$

On the other hand, if $\tau_f \le \tau_r$,

$$Q_L(r_0) = \rho_w L_v \left\{1 - \left[\frac{r(\tau_f)}{r_0}\right]^3\right\}\left(\frac{4\pi r_0^3}{3}\frac{dF}{dr_0}\right), \quad (6b)$$

where $r(\tau_f)$ is the droplet radius at time τ_f,

$$r(\tau_f) = r_{eq} + (r_0 - r_{eq})\exp(-\tau_f / \tau_r). \quad (7)$$

In (6), ρ_w is the density of pure water.

To get the $\overline{Q}_S$ and $\overline{Q}_L$ terms in (4), I integrate (5) and (6) over all droplet sizes relevant to the spray transfer process,

$$\overline{Q}_S = \int_{r_{lo}}^{r_{hi}} Q_S(r_0)\,dr_0, \quad (8a)$$

$$\overline{Q}_L = \int_{r_{lo}}^{r_{hi}} Q_L(r_0)\,dr_0. \quad (8b)$$

Here, r_{lo} and r_{hi} are, nominally, 1 μm and 500 μm, respectively.

Figure 2 shows the results when I apply (4) to the HEXOS data, using the spray generation func-

tion dF/dr_0 from Fairall et al. (1994) (cf. Andreas and DeCosmo 2002). By setting $\alpha = 3.3$, $\beta = 5.7$, and $\gamma = 2.8$, I can explain both the magnitude and the wind-speed dependence in the HEXOS flux data. In other words, as presumed, using microphysical theory and small, non-negative tuning coefficients, I can explain the magnitude and the wind-speed dependence in the HEXOS data as evidence of spray-mediated heat fluxes.

In essence, Fig. 2 shows that I have successfully partitioned the HEXOS measurements of total latent and sensible heat flux, $H_{L,T}$ and $H_{s,T}$, into interfacial contributions, H_L and H_s, and into spray contributions that I represent as

$$Q_{L,sp} = \alpha \overline{Q}_L \ , \qquad (9a)$$

$$Q_{S,sp} = \beta \overline{Q}_S - (\alpha - \gamma)\overline{Q}_L \ . \qquad (9b)$$

We can use the COARE algorithm to estimate H_L and H_s; but rather than the full microphysical calculations, I also want a comparably fast algorithm for predicting $Q_{L,sp}$ and $Q_{S,sp}$.

4. SPRAY FLUX ALGORITHM

Computing $Q_{L,sp}$ and $Q_{S,sp}$ through (5)–(9) is much too involved for any but research applications. Andreas (1992) and Andreas et al. (1995) show, however, that $Q_S(r_0)$ and $Q_L(r_0)$ have dominant peaks at radii of 100 μm and 50 μm, respectively. As a simple parameterization, I therefore postulate that these radii respectively dominate the behaviors of $Q_{S,sp}$ and $Q_{L,sp}$.

In (5), $\tau_f(100\,\mu\text{m}) > \tau_r(100\,\mu\text{m})$. That is, 100-μm droplets have essentially given up all their sensible heat by the time they fall back into the sea. Therefore, I further postulate that

$$Q_{S,sp} = \rho_w c_w (T_s - T_{eq,100}) V_S(u_*) \ , \qquad (10)$$

where $T_{eq,100}$ is the equilibrium temperature in the given ambient conditions of a spray droplet with initial radius 100 μm, and $V_S(u_*)$ is an empirical function of the friction velocity. Andreas and Emanuel (2001) used a similar spray parameterization in their hurricane simulations.

In (6), $\tau_f(50\,\mu\text{m}) < \tau_r(50\,\mu\text{m})$. Therefore, my postulate is

$$Q_{L,sp} = \rho_w L_v \left\{ 1 - \left[\frac{r\left[\tau_f(50\,\mu\text{m})\right]}{50\,\mu\text{m}} \right]^3 \right\} V_L(u_*) \ , \qquad (11)$$

where $r\left[\tau_f(50\,\mu\text{m})\right]$ is the radius at time $\tau_f(50\,\mu\text{m})$ of a droplet with initial radius 50 μm [see (7)], and $V_L(u_*)$ is another empirical function of u_*. Furthermore, I base τ_f on the time required for a droplet with initial radius r_0 to fall one significant wave amplitude, $A_{1/3}$, since droplets of radii 50 μm and 100 μm are probably spume droplets that are blown off the wave crests (Andreas 1992; Andreas and DeCosmo 2002). That is,

$$\tau_f(r_0) = \frac{A_{1/3}}{u_f(r_0)} \ , \qquad (12)$$

where u_f is the terminal fall speed of a droplet with initial radius r_0 (Andreas 1989, 1992), and

$$A_{1/3} = 0.015\left(\frac{u_*}{k}\right)^2 \left\{ 2u_*^2 - u_* \left[2\ln\left(\frac{10\,g}{\alpha_C}\right) + 8 \right] + \left[\left(\ln\left(\frac{10\,g}{\alpha_C}\right) \right)^2 + 2\ln\left(\frac{10\,g}{\alpha_C}\right) + 4 \right] \right\} . \qquad (13)$$

This gives $A_{1/3}$ in meters when u_* is in m s^{-1}. I limit $A_{1/3}$ calculated with (13) to values of 20 m or less.

In Figs. 3 and 4, I test the postulates (10) and (11) using my partitioning of the HEXOS flux data. Both parameterizations seem to collapse the HEXOS spray fluxes well. The plots therefore provide expressions for the empirical velocity functions, which are

$$V_S = 1.65\times10^{-6}\, u_*^3 \ , \qquad (14a)$$

$$V_L = 2.65\times10^{-8}\, u_*^{2.61} \ . \qquad (14b)$$

These give V_S and V_L in m s^{-1} when u_* is in m s^{-1} and, in turn, produce values of $Q_{S,sp}$ and $Q_{L,sp}$ in W m^{-2}.

The procedure for computing the total sensible and latent heat fluxes when given conditions such as U_r, T_r, Q_r, T_s, and Q_s is therefore to first use (1) to compute H_s, H_L, and u_*. Then use this u_* value and (10), (11), and (14) to compute the spray fluxes $Q_{S,sp}$ and $Q_{L,sp}$. Finally, sum these fluxes,

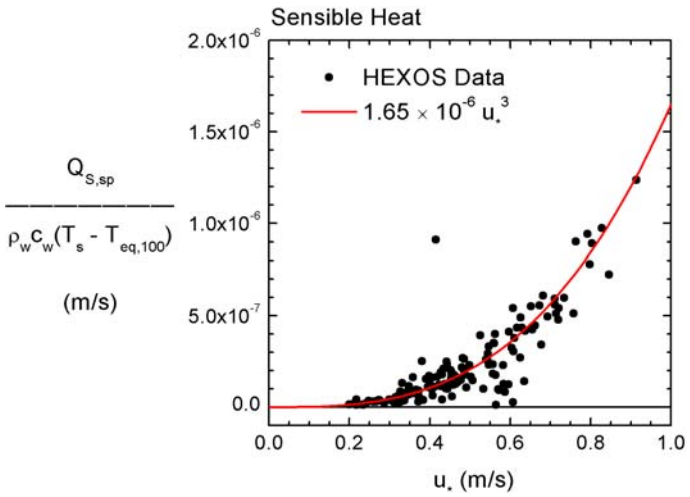

Fig. 3. The spray sensible heat flux, $Q_{S,sp}$, computed from the HEXOS data as (9b) and parameterized as (10). This plot therefore shows $V_S(u_*)$, equation (14a).

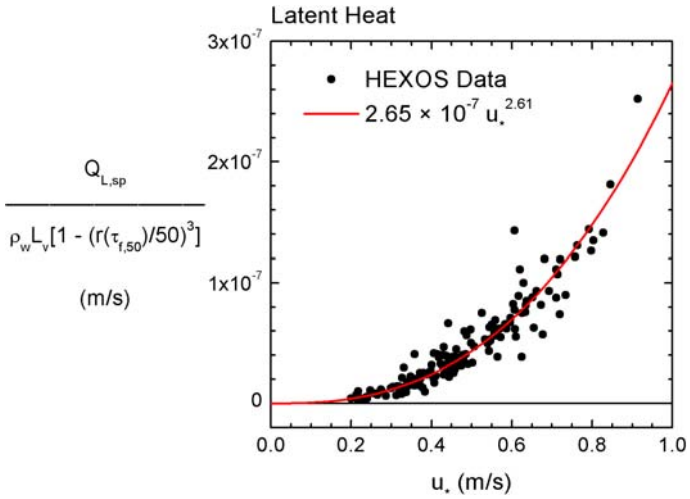

Fig. 4. The spray latent heat flux, $Q_{L,sp}$, computed from the HEXOS data as (9a) and parameterized as (11). Here, $\tau_{f,50}$ is the fall time, (12), of a droplet with initial radius 50 μm. This plot shows $V_L(u_*)$, equation (14b).

$$H_{s,T} = H_s + Q_{S,sp} \quad , \qquad (15a)$$

$$H_{L,T} = H_L + Q_{L,sp} \quad , \qquad (15b)$$

to get the total heat fluxes.

We also need the equilibrium temperature of 100-μm droplets, $T_{eq,100}$, and the equilibrium radius and radius e–folding time of 50-μm droplets, $r_{eq}(50\ \mu m)$ and $\tau_r(50\ \mu m)$, respectively. To create Figs. 3 and 4, I obtained these microphysical quantities by tracking droplet evolution with my full microphysical model. Kepert (1996) and Andreas (1996), however, show how to compute T_{eq} quickly for arbitrary radius and environmental conditions. And as part of this development, I have also formulated comparably fast methods to compute r_{eq} and τ_r for arbitrary radius and conditions. I will report these methods elsewhere.

5. DISCUSSION

To test this spray flux algorithm, I can use (15), instead of my full microphysical model, to model the HEXOS heat fluxes. Figure 5 shows the results.

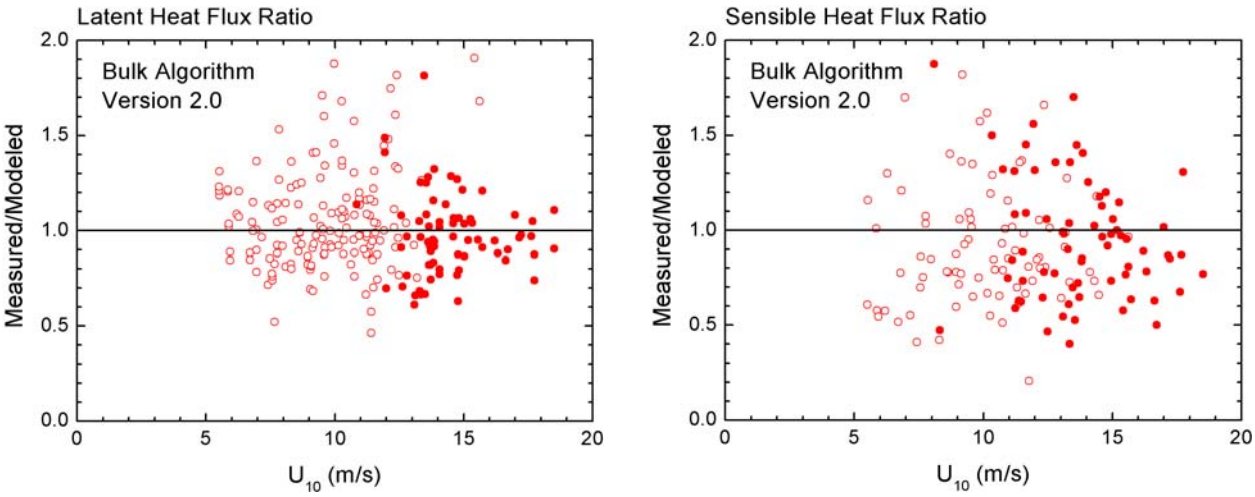

Fig. 5. As in Fig. 2, but here I use the bulk flux algorithm represented by (15) to model the HEXOS latent and sensible heat fluxes. In the latent heat flux panel, the average of the flux ratios is 1.055, and the correlation coefficient with wind speed is 0.001. In the sensible heat flux panel, the ratios average 0.948, and the correlation coefficient is –0.050. In both panels, the filled circles denote cases for which the respective modeled spray flux ($Q_{L,sp}$ or $Q_{S,sp}$) is at least 10% of the modeled interfacial flux (H_L or H_s).

These panels do not look much different than the results with the full microphysical model depicted in Fig. 2. That is, the ratios of measured-to-modeled fluxes in both panels in Fig. 5 average one, and neither plotted ratio depends significantly on wind speed. Moreover, most of the measured HEXOS fluxes for wind speeds above 12 m s^{-1} include at least a 10% spray effect, as also suggested in Fig. 2. Finally, computing fluxes with Version 2.0 of the spray flux algorithm is approximately a hundred times faster than with the full microphysical spray model.

Li et al. (2003) demonstrated that Version 1 of my spray flux algorithm was not sensitive enough to surface temperature because that version assumed $\tau_f(50\,\mu m) >> \tau_r(50\,\mu m)$ in (7) and therefore set $r\left[\tau_f(50\,\mu m)\right]$ in (11) to r_{eq}. Since r_{eq} depends only weakly on temperature, $Q_{L,sp}$ depended only weakly on temperature in Version 1, in contrast to the behavior of the spray latent heat flux reported in Andreas (1992) and Andreas et al. (1995).

With r as a function of τ_f and τ_r in (11), $Q_{L,sp}$ is now appropriately sensitive to temperature because τ_r decreases markedly as temperature increases (Andreas 1990, 1992) while τ_f changes little with temperature. Figure 6 therefore reproduces a plot like Fig. 2 in Li et al. (2003) but now using Version 2.0 of the spray algorithm. Here, $Q_{L,sp}$ now has the strong dependence on temperature reported by Andreas (1992). The upshot is that spray heat transfer should be more important in tropical storms than in high-latitude storms.

Figure 7 likewise demonstrates the algorithm's sensitivity to relative humidity. As the relative humidity increases from 75%, the equilibrium

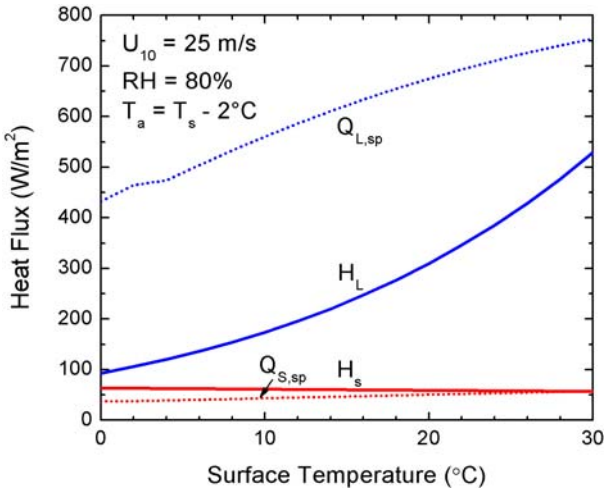

Fig. 6. Sample calculations with Version 2.0 of the bulk flux algorithm to demonstrate the temperature sensitivity. For all calculations, the 10-m wind speed U_{10} was 25 m s^{-1}, the relative humidity RH was 80%, the air temperature was 2°C less than the surface temperature (i.e., $T_a = T_s - 2°C$), the barometric pressure was 1000 mb, and the surface salinity was 34 psu.

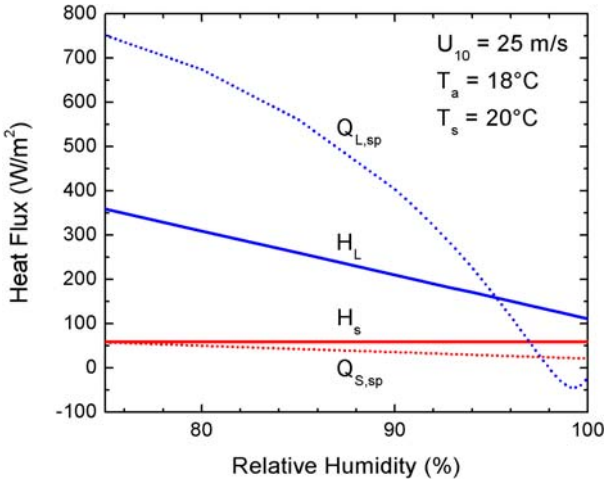

Fig. 7. Sample calculations with the bulk flux algorithm to demonstrate its humidity sensitivity. Conditions are as in Fig. 6, except here the relative humidity varies, the air temperature T_a is 18°C, and the surface temperature is 20°C.

radius of droplets that started at 50 μm moves progressively closer to 50 μm. In other words, as the relative humidity increases, the droplets have less potential for giving up water vapor, and $Q_{L,sp}$ gets progressively smaller. Once the relative humidity is higher than the saturation value for seawater—typically about 98% for seawater of salinity 34 psu—water actually begins condensing on these 50-μm droplets. They, thus, become a sink for latent heat, and $Q_{L,sp}$ goes negative. Version 2.0 of the algorithm does not allow humidities above 100%, and it is hard to imagine how the humidity in the marine boundary layer can get much above the seawater-saturation value, 98%.

6. SUMMARY

I have developed a fast bulk flux algorithm for high-wind, spray conditions. In essence, the spray part of the algorithm simplifies Andreas's (1989, 1992) microphysical spray model. The algorithm predicts the interfacial fluxes with a standard bulk flux algorithm that uses the COARE Version 2.6 expressions for the roughness lengths z_0, z_T, and z_Q.

I can provide you an executable version of this algorithm if you would like to try it out. Alternatively, I will gladly share the full FORTRAN code if you would like to embed it in your specific application. Perrie et al. (2004a, 2004b) and Li et al. (2003) have used Version 1.1 of this algorithm in their simulations of extratropical storms and demonstrate that accounting for spray effects improves storm simulations.

7. ACKNOWLEDGMENTS

I thank Will Perrie of Bedford Institute for the impetus he has provided. The U.S. National Science Foundation supported this work with award ATM-00-01037; the U.S. Office of Naval Research supported it with award N0001404MP20091.

8. REFERENCES

Andreas, E. L, 1989: Thermal and size evolution of sea spray droplets. CRREL Report 89-11, U.S. Army Cold Regions Research and Engineering Laboratory, Hanover, NH, 37 pp.

_____, 1990: Time constants for the evolution of sea spray droplets. *Tellus*, **42B**, 481–497.

_____, 1992: Sea spray and the turbulent air-sea heat fluxes. *J. Geophys. Res.*, **97**, 11,429–11,441.

_____, 1995: The temperature of evaporating sea spray droplets. *J. Atmos. Sci.*, **52**, 852–862.

_____, 1996: Reply. *J. Atmos. Sci.*, **53**, 1642–1645.

_____, 2003: An algorithm to predict the turbulent air-sea fluxes in high-wind, spray conditions. Preprints, *12th Conf. on Interactions of the Sea and Atmosphere*, Long Beach, CA, Amer. Meteor. Soc., CD-ROM 3.4, 7 pp.

_____, 2004: Spray stress revisited. *J. Phys. Oceanogr.*, **34**, 1429–1440.

_____, and J. DeCosmo, 1999: Sea spray production and influence on air-sea heat and moisture fluxes over the open ocean. *Air-Sea Exchange: Physics, Chemistry and Dynamics*, G. L. Geernaert, Ed., Kluwer, 327–362.

_____, and ____, 2002: The signature of sea spray in the HEXOS turbulent heat flux data. *Bound.-Layer Meteor.*, **103**, 303–333.

_____, and K. A. Emanuel, 2001: Effects of sea spray on tropical cyclone intensity. *J. Atmos. Sci.*, **58**, 3741–3751.

_____, and G. Treviño, 2000: Comments on "A physical interpretation of von Kármán's constant based on asymptotic considerations—A new value." *J. Atmos. Sci.*, **57**, 1189–1192.

_____, J. B. Edson, E. C. Monahan, M. P. Rouault, and S. D. Smith, 1995: The spray contribution to net evaporation from the sea: A review of

recent progress. *Bound.-Layer Meteor.*, **72**, 3–52.

DeCosmo, J., 1991: Air-sea exchange of momentum, heat and water vapor over whitecap sea states. Ph.D. dissertation, University of Washington, 212 pp. [Available from UMI Dissertation Services, P. O. Box 1346, Ann Arbor, MI 48106–1346.]

_____, K. B. Katsaros, S. D. Smith, R. J. Anderson, W. A. Oost, K. Bumke, and H. Chadwick, 1996: Air-sea exchange of water vapor and sensible heat: The Humidity Exchange over the Sea (HEXOS) results. *J. Geophys. Res.*, **101**, 12,001–12,016.

Emanuel, K. A., 2003: A similarity hypothesis for air-sea exchange at extreme wind speeds. *J. Atmos. Sci.*, **60**, 1420–1428.

Fairall, C. W., J. D. Kepert, and G. J. Holland, 1994: The effect of sea spray on surface energy transports over the ocean. *Global Atmos. Ocean Sys.*, **2**, 121–142.

_____, E. F. Bradley, D. P. Rogers, J. B. Edson, and G. S. Young, 1996: Bulk parameterization of air-sea fluxes for Tropical Ocean-Global Atmosphere Coupled-Ocean Atmosphere Response Experiment. *J. Geophys. Res.*, **101**, 3747–3764.

Garratt, J. R., 1992: *The Atmospheric Boundary Layer*. Cambridge University Press, 316 pp.

Johnson, H. K., J. Højstrup, H. J. Vested, and S. E. Larsen, 1998: On the dependence of sea surface roughness on wind waves. *J. Phys. Oceanogr.*, **28**, 1702–1716.

Katsaros, K. B., and J. DeCosmo, 1990: Evaporation in high wind speeds, sea surface temperature at low wind speeds, examples of atmospheric regulation. *Modelling the Fate and Influence of Marine Spray*, P. G. Mestayer, E. C. Monahan, and P. A. Beetham, Eds., Marine Sciences Institute, University of Connecticut, Groton, 106–114.

Kepert, J. D., 1996: Comments on “The temperature of evaporating sea spray droplets.” *J. Atmos. Sci.*, **53**, 1634-1641.

Li, W., W. Perrie, E. L Andreas, J. Gyakum, and R. McTaggart-Cowan, 2003: Impact of sea spray on numerical simulation of extratropical hurricanes. Preprints, *12th Conf. on Interactions of the Sea and Atmosphere*, Long Beach, CA, Amer. Meteor. Soc., CD-ROM 2.5, 9 pp.

Perrie, W., E. L Andreas, W. Zhang, W. Li, J. Gyakum, and R. McTaggart-Cowan, 2004a: Sea spray impacts on intensifying midlatitude cyclones. *J. Atmos. Sci.*, submitted.

Perrie, W., W. Zhang, Z. Long, and E. L Andreas, 2004b: Impacts of waves, sea spray, and the upper ocean on extratropical storms. Preprints, *13th Conf. on Interactions of the Sea and Atmosphere*, Portland, ME, Amer. Meteor. Soc., CD-ROM 8.5, this volume.

Smith, S. D., 1988: Coefficients for sea surface wind stress, heat flux, and wind profiles as a function of wind speed and temperature. *J. Geophys. Res.*, **93**, 15,467–15,472.

Wu, J., 1982: Wind-stress coefficients over sea surface from breeze to hurricane. *J. Geophys. Res.*, **87**, 9704–9706.

Zilitinkevich, S. S., 1969: On the computation of the basic parameters of the interaction between the atmosphere and the ocean. *Tellus*, **21**, 17–24.